

Title:

Static and Fatigue Behavior of a Carbon-Fiber SMC-R Composite under Combined Tensile and Shear Stresses

Authors:

1. **Given name:** Monish, **family name:** Urapakam Ramakrishnan^{a b}

Email: mramakri@umich.edu

2. **Given name:** Pankaj, **family name:** Mallick^a

Email: pkm@umich.edu

^a Department of Mechanical Engineering, University of Michigan-Dearborn, 4901 Evergreen Rd., Dearborn, MI 48128, USA.

^b Corresponding author.

This is the author manuscript accepted for publication and has undergone full peer review but has not been through the copyediting, typesetting, pagination and proofreading process, which may lead to differences between this version and the Version of Record. Please cite this article as doi: [10.1002/pc.26545](https://doi.org/10.1002/pc.26545)

This article is protected by copyright. All rights reserved.

Abstract

Randomly oriented short fiber reinforced sheet molding compound composites (SMC-R) are among the most commonly used composites for automotive and many non-automotive structural applications. Many studies have reported the static and fatigue properties of SMC-R composites under uniaxial stress conditions. However, there are many applications in which they may be subjected to biaxial stress conditions and their biaxial properties have not been reported in literature. The current study considers the static and fatigue characteristics of a randomly oriented carbon fiber SMC-R under both uniaxial and biaxial loading conditions with various combinations of tensile and shear stresses. A butterfly shaped Arcan specimen was used to conduct the biaxial stress tests. Since both static strength and fatigue life data exhibited significant variability, statistical analysis was conducted using Weibull distribution to analyze the variations in these properties of the material. In biaxial conditions in which a shear stress is imposed along with a tensile stress, the tensile strength of the material decreases with increasing shear stress. A failure envelope drawn based on von Mises equation shows reasonable agreement with the experimental results. As a percentage of the static strength, the fatigue strengths at 1 million cycles in tension and combined equal tension and shear are significantly higher than the fatigue strength in pure shear.

Keywords: Carbon fiber SMC, biaxial loading, static strength, fatigue strength, Weibull distribution.

1 Introduction

Sheet molding compounds with randomly oriented short fibers (SMC-R) are a low cost, lightweight composite alternative to conventional materials in many structural and semi-structural automotive, aerospace, and other industrial applications. They exhibit relatively high modulus-to-

density and strength-to-density ratios, and a planar isotropic characteristic. The compression molding process for transforming flat SMC-R sheets to complex composite parts is now well established. The quasi-static behavior, damage development and uniaxial fatigue response of glass fiber SMC-R are also well documented in literature ^[1-9]. The interest in carbon fiber SMC-R is more recent and studies on their mechanical properties and processing characteristics are relatively few.

Carbon fiber SMC-R has lower density, higher modulus-to-density and strength-to-density ratios compared to glass fiber SMC-R and therefore, a higher weight saving potential in structural applications. For this reason, interest in carbon fiber SMC-R has grown recently in both automotive and aerospace industries and has led to several research studies that started with Feraboli et al. ^[10, 11] who used prepreg-based carbon fiber SMC-R in their study. In their study, unidirectional continuous carbon fiber prepreps are cut into chips of discontinuous lengths that are then dispersed in a randomly distributed fashion in a mold and compression molded into the final shape. The molded material can show a two-dimensional isotropic behavior if there is limited flow in the mold. Feraboli et al. ^[10] observed that the tensile, compressive, and flexural strengths of carbon fiber chip reinforced epoxy SMC-R increased with chip length as well as chip length-to-width ratio; however, the modulus values remained nearly independent of chip length. In tension tests, specimen failure occurred by delamination through the thickness in the form of separation of multiple chips in a single stack. Stelzer et al. ^[12] conducted tension-tension, tension-compression and compression-compression fatigue tests on 50-mm long carbon fiber chip reinforced epoxy SMC-R that was also prepared with relatively low flow in the mold and observed large scatter in the fatigue data, particularly in tension-tension mode.

Martuli et al. ^[13] investigated the effect of in-mold flow on the tensile properties of a carbon

fiber chip reinforced vinyl ester SMC-R. The compression molded plates were made with 20% initial mold coverage, allowing flow to take place over 80% of the mold. Since the initial SMC-R material was placed over only 20% surface area of the mold, when molding pressure was applied, it flowed across the remaining 80% to fill the mold cavity. This caused the short fibers in the SMC-R to rotate from their random orientation to become more aligned in the direction of flow in the mold. This flow-induced fiber orientation resulted in significant differences in tensile properties in the 0, 45 and 90° directions relative to the direction of flow. For example, in the flow or 0° direction, the average tensile strength was 255 MPa, while normal to the flow direction or 90° direction, the average tensile strength was 71 MPa. In tension-tension fatigue tests reported by Martuli et al. ^[14], there were also significant differences in fatigue life diagrams in these three directions, although when the fatigue strength was normalized by dividing with respective tensile strength, the differences became relatively small. Large scatters in both static and fatigue data were attributed to spatial variation of fiber orientation in the molded plates. Pre-failure scan of fatigue specimens showed evidence of inter-tow splitting along the longitudinal axes of tows by a combination of debonding and matrix cracking, but the tow ends acted as a barrier to inter-tow in-plane crack propagation. Instead, cracks propagated mainly in the thickness direction.

Another series of quasi-static and fatigue studies on carbon fiber chip reinforced SMC-R composites were reported by Tang et al. ^[15, 16]. In these studies, the compression-molded plate was found to be planar isotropic; however, due to spatial variation of fiber orientations, there were significant scatters in both tensile, compressive and fatigue strengths of the material. For example, the tensile strength varied between 200 to 273 MPa and the compressive strength varied between 234 to 316 MPa. It was shown that variations in local fiber orientations caused spatial variation in the modulus of the material. Linear relationships were observed between the failure strengths

and the local modulus at the failure location. Scatters in static and fatigue test data were attributed to spatial variation of fiber orientations in the material. The fatigue failure modes included matrix cracking, chip edge debonding from the matrix, and chip splitting.

One study in which carbon fiber SMC-R was prepared using the conventional SMC sheet making process that involves randomly dispensed chopped carbon fiber tows between two layers of a thermosetting polymer was due to Nony-Davadie et al. ^[17]. In this study, two different mold coverages were used in compression molding the SMC-R plates, one to produce random orientation of fibers in the molded plate and the other to produce a preferential orientation of fibers in the flow direction. They observed that there was angular dependence of mechanical properties in both cases. Even in the plates with random fiber orientation, the tensile modulus and strength were higher in the 0° direction, which was identified as the direction of fiber deposition direction during the sheet making process. In plates with preferential orientation of fibers, the tensile strength and modulus were significantly higher in the 0° direction which was identified as the material flow direction during compression molding. Nony-Davadie et al. also reported the uniaxial tension-tension fatigue behavior of the carbon fiber SMC-R and observed a high degree of variability in fatigue life. In both static and fatigue specimens, a two-stage failure process was observed, first by the formation of inter-bundle damage in the form of fiber pull-out, debonding and matrix cracking inside the bundle and then by the formation of large cracks that led to the final failure.

In the experiments conducted by Sieberer et al. ^[18], carbon fiber SMC-R plates were compression molded using a material prepared by depositing 25.4 mm long chopped carbon fiber tows on a moving belt covered with an epoxy resin. The average compressive strength of the material was found to be higher than the average tensile strength of the material and there was

little difference in the strength values of the specimens oriented at 0 and 90° directions to the fiber deposition direction. The fatigue data in completely reversed fatigue cycling showed considerable scatter; but the difference between statistically regressed stress-life lines for the 0 and 90° specimens was not very significant. Modulus degradation during fatigue cycling also showed large variability; however, in general, after an initial degradation within the first 10% of the fatigue life, the change in modulus was very moderate until about 90% of the fatigue life when the modulus decreased very rapidly as the specimens failed.

All of the previous studies on the fatigue behavior of glass fiber and carbon fiber SMC-R involved uniaxial loading. In the present study, experiments were conducted to determine the quasi-static and fatigue behavior of a carbon fiber SMC-R under uniaxial and combined cyclic loading conditions. A modified butterfly shaped Arcan specimen capable of inducing both uniaxial as well as combined loading on the specimen was used. The combined loading condition includes a combination of tensile and shear stresses. The original Arcan specimen was developed by Arcan and his co-workers ^[19, 20] to study the in-plane characteristics of composite laminates under biaxial loads. A combination of tensile or compressive and shear loads can be applied to the specimen in this test and the biaxiality ratio can be varied by changing the orientation of the critical section of the specimen with respect to the loading axis. The principal advantages of the Arcan test method over other biaxial test methods for composites are that it can be applied to flat composite plate specimens, and it can be conducted on a uniaxial testing machine without the use of expensive equipment or fixtures. The butterfly shaped Arcan specimens were used to study the biaxial behavior of unidirectional glass fiber composites ^[21, 22] and an E-glass fiber SMC-R composite ^[23] under combined tensile and shear loadings.

2 Experimental Method

A carbon fiber SMC-R supplied by Quantum Composites, a division of A. Schulman, is the material considered for this experimental study. The material consists of chopped carbon fibers in an epoxy matrix with a fiber weight fraction of 52%. A mix of 25 mm and 50 mm long chopped 3K-PAN carbon fibers was used. For good moldability, the chopped fiber length in a typical sheet molding compound is 25 mm. In the material considered here, both 25 mm and 50 mm long chopped fibers were used to maintain good moldability and to improve its tensile strength. The SMC-R sheet was prepared using a conventional SMC machine and a stack of three layers of the sheet were compression molded to obtain the final dimensions of 300 mm x 300 mm x 3.18 mm (thickness). The basic mechanical properties of the material as provided by the material supplier are listed in Table 1. They were determined using standard uniaxial tensile, flexural and compression tests of specimens machined from 300 mm x 300 mm panels molded with 80% mold coverage, 70 bar pressure, and 138-149°C temperature for 6-10 minutes.

Table 1: Properties of carbon fiber SMC-R ⁽¹⁾ used in the study

Property	Value
Density	1.45 g/cm ³ .
Tensile Modulus	37.92 GPa
Tensile Strength	290 MPa
Compressive Stress (at break)	276 MPa

⁽¹⁾ As reported by the material supplier, Quantum Composites

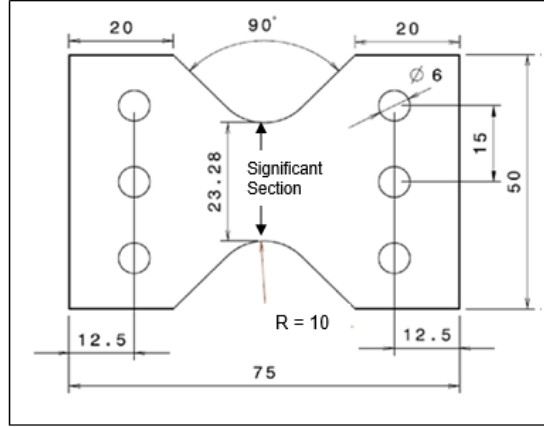


Figure 1: Arcan specimen dimensions (Dimensions are in mm)

Both static and fatigue experiments were conducted using a butterfly shaped Arcan specimen shown in Figure 1. It contains two opposing 90° notches with 10 mm radius at its mid-length and external dimensions of 75 mm x 50 mm. The region between the notches is called the significant section. The specimen dimensions were determined after conducting a parametric dimensional study using the ABAQUS finite element software to create a nearly uniform stress distribution across the significant section [24]. The experimental work was carried out on an MTS 210 servo-hydraulic testing machine. The butterfly shaped Arcan specimen was clamped onto a circular test fixture (Figure 2) containing two front and two back split steel plates on which a series of bolt holes are drilled at 15° intervals to hold the test specimens at different orientations with respect to the vertical loading direction. The circular fixture is mounted on the testing machine using three pins at both fixed and moving ends of the loading anvils. By mounting the specimens at different loading angles (θ) with respect to the loading axis (Figure 2), the loading condition on the specimen can be varied from uniaxial tension at $\theta = 0^\circ$, combined tension and shear at $0^\circ < \theta < 90^\circ$, and pure shear at $\theta = 90^\circ$.



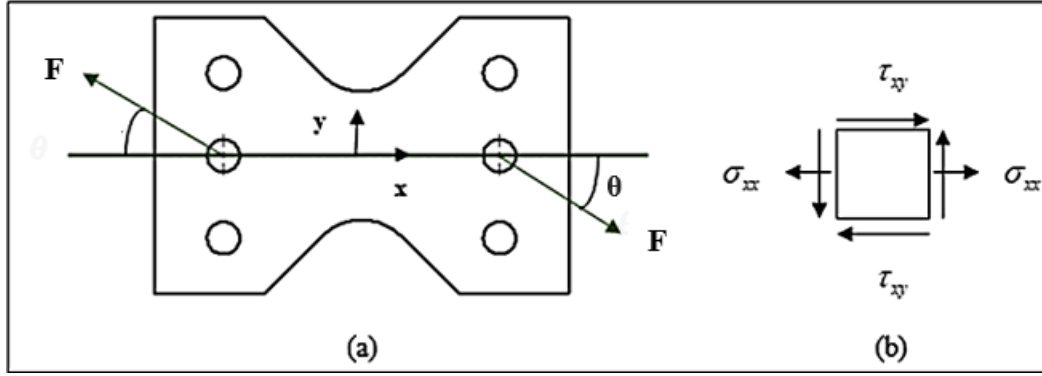
Figure 2: Modified Arcan specimen mounted on the MTS testing machine

A schematic representation of load F acting on a test specimen at a loading angle θ , along with a stress element in the significant section, is shown in Figure 3 (a). The average nominal stresses in the significant section of the specimen are given by Equation (1).

$$\sigma_{xx} = \frac{F_x}{A} = \frac{F \cos \theta}{A}, \quad \sigma_{yy} = 0$$

$$\tau_{xy} = \frac{F_y}{A} = \frac{F \sin \theta}{A} \quad (1)$$

It can be observed in this equation that as the loading angle is increased, the tensile stress component decreases and the shear stress component increases. For $\theta = 0^\circ$, the only nominal stress in the significant section is the normal tensile stress σ_{xx} , and for $\theta = 90^\circ$, the only nominal stress is the shear stress τ_{xy} . For $\theta = 45^\circ$, both σ_{xx} and τ_{xy} are present; they are both equal to $0.707 (F/A)$ in magnitude. At this loading angle, a biaxial tension-compression normal stress condition is created due to the principal stresses that are $1.144 (F/A)$ and $-0.437(F/A)$. Similar biaxial tension-compression principal stress conditions also exist at loading angles other than 0 and 90° .



Quasi-static experiments were conducted at a crosshead speed of 2 mm/min to obtain the static strengths of the material at $\theta = 0, 30, 45, 60$ and 90° . At least four specimens were tested at each loading angle. Uniaxial tension, equal tension and shear, and pure shear fatigue experiments were conducted in load-controlled mode at $\theta = 0^\circ, 45^\circ$ and 90° , respectively. The minimum-to-maximum cyclic load ratio (R) was 0.1 and the fatigue life run out was set at 1 million cycles. Initially, several uniaxial tension fatigue tests were conducted using a frequency of 2 Hz. Seven of the 10 specimens tested at this frequency exceeded a life of 200,000 cycles and did not fail at 91% or below of the static strength. Further fatigue tests at this frequency were discontinued due to long test times. The remaining fatigue tests were conducted at a higher frequency of 10 Hz. The total number specimens tested at this frequency was 57 that included 27 specimens at 0° loading angle, 15 specimens at 45° loading angle, and 15 specimens at 90° loading angle. The cyclic load and displacement data were recorded at a frequency of 100 Hz. Both static and fatigue test specimens were taken from various locations of different plates in the same direction with respect to a reference marking on the plates and were tested in a random order.

3 Results

3.1 Static Tests

The quasi-static tests were conducted to determine the load-displacement characteristics of the material under different uniaxial and biaxial loading conditions. The 0 and 90° loading angles create uniaxial tensile and pure shear stresses in the center of the significant section, respectively, while 30, 45 and 60° loading angles create different biaxial stress conditions in the specimen's significant section. Figure 4 compares typical load vs. displacement curves for the different loading conditions considered. The load-displacement curves in this figure show the presence of a knee or a break, which is considered the load at the onset of damage in the specimen being tested. After the peak load is reached, the load on the specimen decreases in steps until the entire specimen fails. Another observation to be made from Figure 4 is that the carbon fiber SMC-R considered in this study shows a significant decrease in peak loads as the loading angle is increased from 0 to 45°. However, between 45 and 90° loading angles, changes in peak loads are relatively small.

The normal and shear stress components corresponding to the peak loads at different loading angles θ are plotted in Figure 5. The stress values were calculated using Equation 1. The plot of normal stress σ_{xx} vs. shear stress τ_{xy} shows a quadratic nature of the effect of biaxiality on the material. The normal stresses at peak and knee loads are observed to decrease with increase in shear stress in the significant section. The normal stress corresponding $\theta = 0^\circ$ represents the tensile strength of the material, whereas the shear stress corresponding to $\theta = 90^\circ$ represents the shear strength of the material. The quadratic nature of σ_{xx} vs. τ_{xy} indicates that the tensile strength of the carbon fiber SMC-R decreases in presence of a shear stress. Conversely, it also indicates that the shear strength of the material decreases in presence of a tensile stress. Similar relationships were observed previously for an E-glass fiber SMC-R [23].

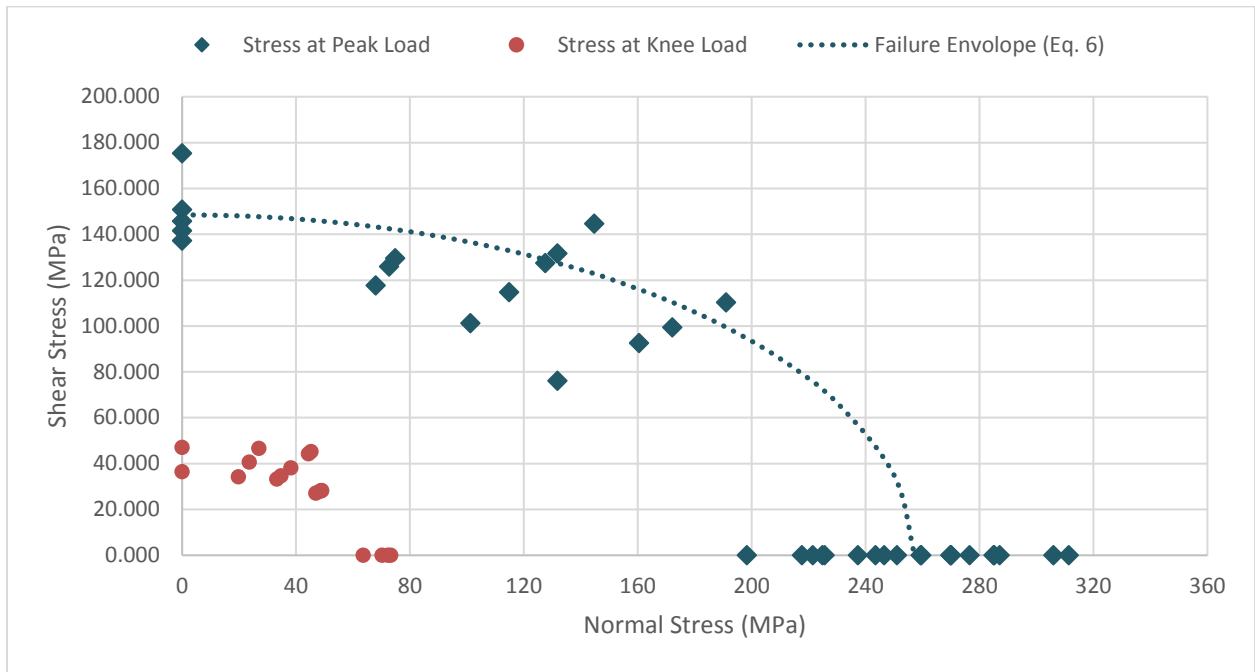
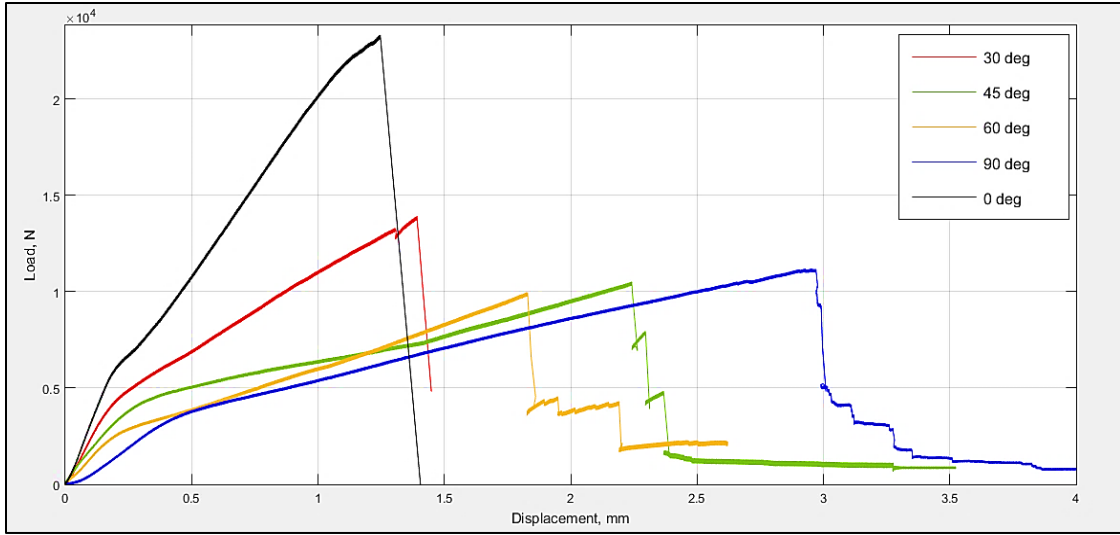


Figure 5: Normal stress σ_{xx} vs. shear stress τ_{xy} corresponding to peak and knee loads at various loading angles for the carbon fiber SMC-R

Figure 5 shows that there is large amount of scatter in peak normal and shear stresses observed in the static tests. For example, with 0° loading angle, the peak tensile stress ranged from 198.3 MPa to 311.4 MPa. At 45° loading angle, the peak normal and shear stresses ranged from

101.2 MPa to 144.7 MPa. At 90° loading angle, corresponding to pure shear, the peak shear stress ranged from 137.2 to 175.3 MPa. Since fatigue tests were performed at 0, 45 and 90° loading angles, it was decided to explore the nature of the variation in peak static stresses and the corresponding static strengths for these three loading angles using a 2-parameter Weibull analysis [25].

The Weibull plots with the probability of failure along the vertical axis and the peak tensile stress along the horizontal axis are shown in Figure 6. For a 2-parameter Weibull distribution, the mean peak stress is defined as:

$$S_t = S_o \Gamma \left(\frac{1+\alpha}{\alpha} \right) \quad (2)$$

where, S_t is the mean peak stress or the static strength (in MPa), S_o is the scale parameter (also in MPa), and α is the dimensionless shape parameter. To calculate the scale and shape parameters, the probability of failure (P) was calculated using the mean rank given by Equation (3) and then using the methodology given in Reference [25].

$$P = \frac{i}{1+n} \quad (3)$$

where, n = total number of specimens tested and i = rank in the order of increasing peak stress value. Results of the Weibull analysis are listed in Table 2. Using the Weibull analysis, the mean values of the static strengths at 0, 45 and 90° loading angles were determined as 257.2, 123.9 and 150.1 MPa. The static strengths at 0 and 90° loading angles represent the tensile strength and shear strength of the material. It is to be noted that the mean tensile strength determined using the Arcan specimen is 257.2 MPa compared to 290 MPa determined using uniaxial tensile specimens (See Table 1).

Since SMC-R composites are planar isotropic (because of random fiber orientation in the

plane of the composite plate), the traditional failure criteria for continuous fiber composites, such as Azzi-Tsai-Hill criterion [26], may not be applicable to predict their failure strength. Urapakam Ramakrishnan and Mallick [23] applied a quadratic failure criterion proposed by Hill [27] for anisotropic materials to represent the biaxial strength behavior of a glass fiber SMC-R. The Hill equation given by Equation (2) takes into consideration the through-thickness anisotropy in the material and introduces two anisotropy ratios R and P in the principal stress coordinates.

$$\left[\frac{R}{(1+R)}(\sigma_1 - \sigma_2)^2 + \frac{R}{P(1+R)}\sigma_2^2 + \frac{1}{(1+R)}\sigma_1^2 \right]^{1/2} = S \quad (2)$$

In Equation (2), σ_1 and σ_2 are the in-plane principal stresses corresponding to the failure load, and S is the uniaxial tensile strength of the material. For a planar isotropic material, $R = P$, and Equation (2) transforms into Equation (3) given below.

$$\left[\sigma_1^2 - \frac{2R}{(1+R)}\sigma_1\sigma_2 + \sigma_2^2 \right]^{1/2} = S \quad (3)$$

Note that for $R = P = 1$, Equation (4) transforms into the classical von Mises Equation given by Equation (4) that is commonly used for predicting yielding in isotropic materials under biaxial stresses.

$$\left[\sigma_1^2 - \sigma_1\sigma_2 + \sigma_2^2 \right]^{1/2} = S \quad (4)$$

Urapakam Ramakrishnan and Mallick [23] observed that for the glass fiber SMC-R composite, Equation (4) matches reasonably well with the experimental data. Equation (4) is also applied in this study for carbon fiber SMC-R in the following manner.

If $\sigma_{yy} = 0$, as is the case in the Arcan specimens, the in-plane principal stresses σ_1 and σ_2 can be written in terms of σ_{xx} and τ_{xy} as

$$\sigma_1 = \frac{1}{2} \left[\sigma_{xx} + \sqrt{\sigma_{xx}^2 + 4\tau_{xy}^2} \right], \quad \sigma_2 = \frac{1}{2} \left[\sigma_{xx} - \sqrt{\sigma_{xx}^2 + 4\tau_{xy}^2} \right] \quad (5)$$

In terms of σ_{xx} and τ_{xy} , Equation (4) can then be written as

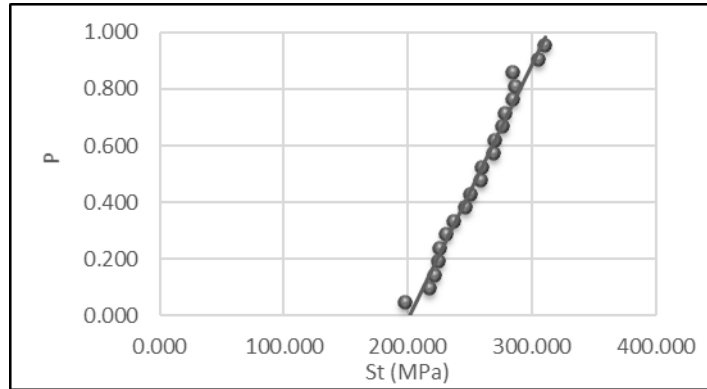
$$\left[\sigma_{xx}^2 + 3\tau_{xy}^2 \right]^{1/2} = S \quad (6)$$

Equation (6) represents a quadratic equation in the $\sigma_{xx} - \tau_{xy}$ space. With S as the mean tensile strength, which is equal to 257.2 MPa for the carbon fiber SMC-R, Equation (6) is plotted in Figure 5, and despite the scatter in the experimental data, a reasonable agreement is found. Using Equation (6), the static strength in shear is calculated as 148.5 MPa, which is 58% of the static strength in tension and only 1% lower than the experimental mean value. Similarly, the static strength in equal tension and shear is 128.6 MPa and only 3.8% higher than the experimental mean value.

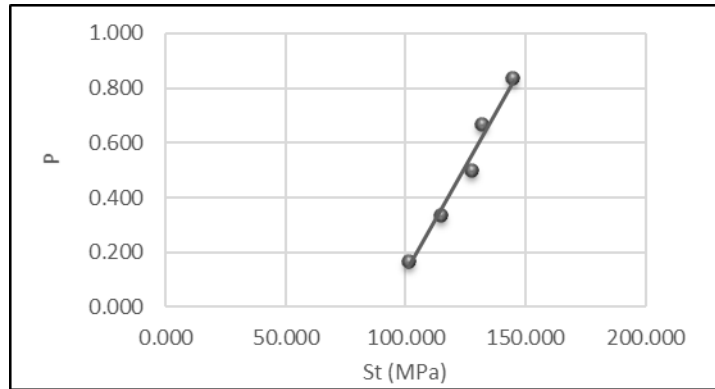
Table 2: Static strengths of carbon fiber SMC-R composite at three different loading angles

Loading Angle (°)	Mode of Loading	No. of Specimens	Range of Peak Stresses (MPa)	Weibull Parameters ⁽¹⁾		Static Strength (Mean Peak Stress) (MPa)
				α	S_o (MPa)	
0	Uniaxial Tension	20	198.3-311.4	8.734	270.951	257.2
45	Equal Tension and Shear	5	101.2-144.7	6.431	132.168	123.9
90	Pure Shear	5	137.2-175.3	8.239	158.216	150.1

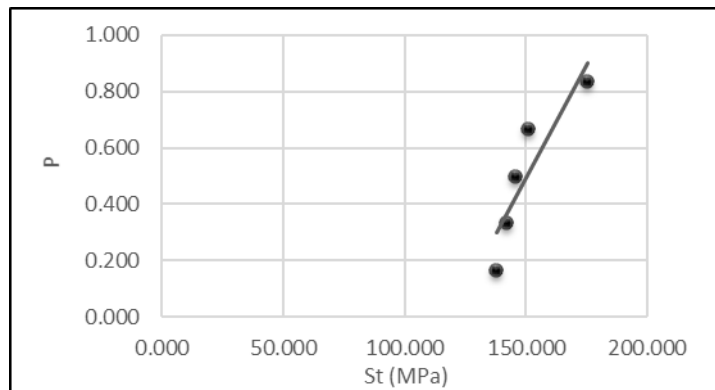
⁽¹⁾ α = Shape parameter and S_o = Scale parameter



(a) 0° loading angle



(b) 45° loading angle



(c) 90° loading angle

Figure 6: Probability of failure (P) vs. static strength (S_t) of carbon fiber SMC-R composite

MPa to 220 MPa. At 220 MPa, which is 86% of the static strength, two specimens failed in less than 5 cycles, while the third specimen failed at 97,800 cycles. Subsequent fatigue tests were conducted on 24 specimens at different maximum stress levels ranging from 100 and 200 MPa. No failure was observed for six specimens in 1 million cycles below a maximum cyclic stress level of 180 MPa or 70% of the static strength. At 190 and 200 MPa maximum cyclic stress levels (corresponding to 74 and 78% of the static strength, respectively), fatigue life ranged from 945 cycles to over 1 million cycles. At 190 MPa, 4 out of 6 specimens, and at 200 MPa, 4 out of 12 specimens did not fail in 1 million cycles. There was no major difference in the variation of fatigue life for specimens taken from different plates.

Under biaxial fatigue with 45° loading angle that produces equal tensile and shear stresses, no failure was observed in 5 specimens at a maximum stress of 80 MPa which is 65% of the static strength in 1 million cycles. Three of the five specimens tested at 100 MPa or 81% of the static strength failed in the range of 108,138 to 552,673 cycles, while two specimens did not fail in 1×10^6 cycles. All five specimens tested at 110 MPa or 88.8% of the static strength failed and the fatigue life ranged from 274 to 373,317 cycles.

In the case of shear fatigue tests with 90° loading angle, failure was observed at 406,600 cycles in one out of four tests at a maximum cyclic stress of 80 MPa, which is 53.3% of the static strength; none of the other specimens failed. Failure was observed in two tests at 25,500 and 63,503 cycles at 100 MPa or 67% of the static strength, while three other specimens reached the run-out limit of 1 million cycles. At 110 MPa or 73.3% of the static strength, four of the five specimens tested failed in the range of 8,108 to 509,482 cycles, while one specimen did not fail in 1×10^6 cycles. Experiments at higher cyclic stress were excluded as the maximum stress would be very close to the static strength of the material.

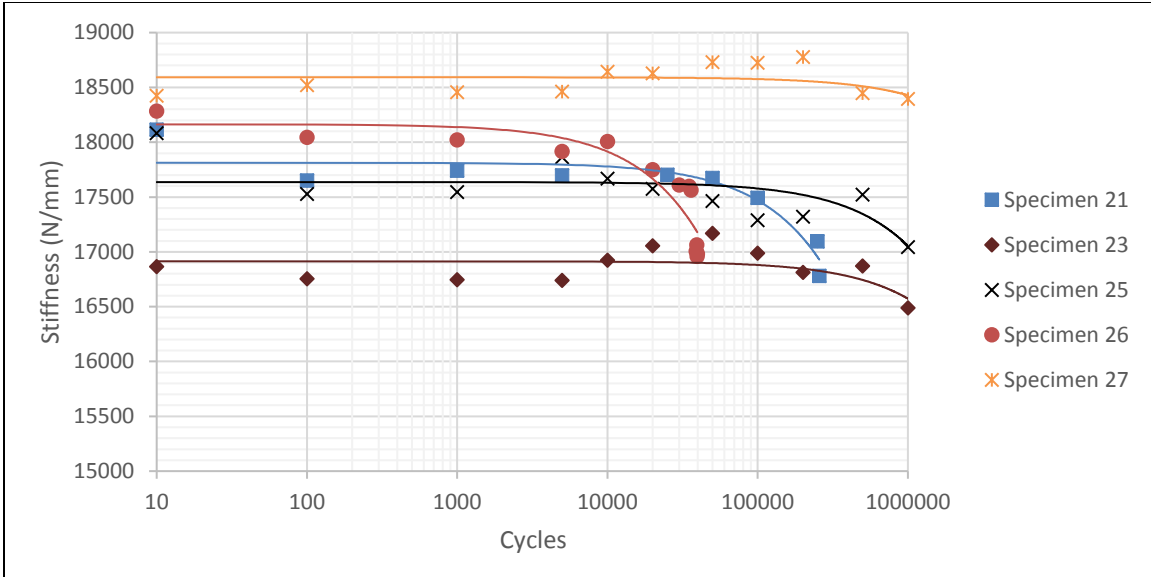


Figure 8: Stiffness variation in 5 fatigue specimens, all tested at 200 MPa maximum cyclic stress. The loading angle is 0°.

Figure 8 plots the stiffness (calculated as the ratio of the maximum load and the maximum displacement) vs. fatigue cycles under tension-tension fatigue load for five specimens at 0° loading angle and a maximum cyclic stress of 200 MPa. The stiffness results also indicate a variability in fatigue performance. Specimens 21 and 26 which failed 2.571×10^5 and 39,650 cycles respectively show a sudden decrease in stiffness just prior to failure. Specimens 23, 25 and 27 did not fail in 1×10^6 cycles and show a gradual decrease in stiffness over the duration of fatigue cycling. The variance in the stiffness behavior is probably a result of the variance in the fiber distributions and orientations at the significant sections in different specimens.

Figure 9 shows photographs of failed fatigue specimens tested at 0, 45 and 90° loading angles. The 0°-specimen, which was in uniaxial tension, failed in the significant section. The 45°-specimen under combined equal tension and shear stresses and the 90°-specimen under pure shear stress failed slightly away from the significant section.



(a) Uniaxial Tension – 0° Loading Angle



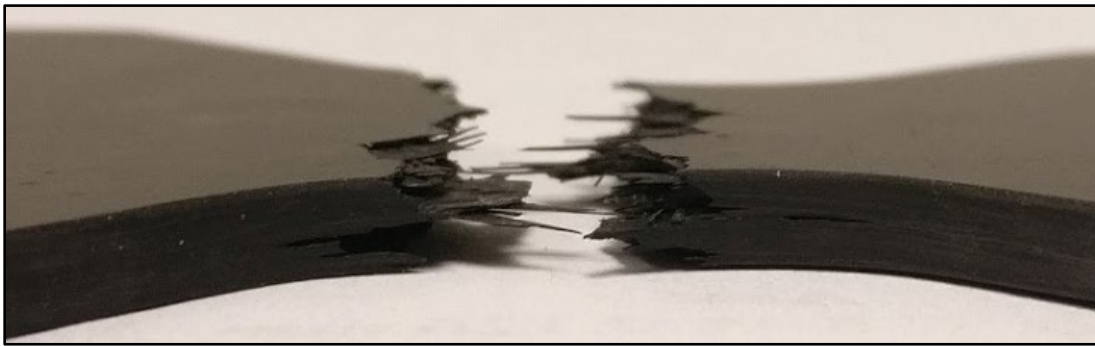
(b) Combined Tension and Shear – 45° Loading Angle



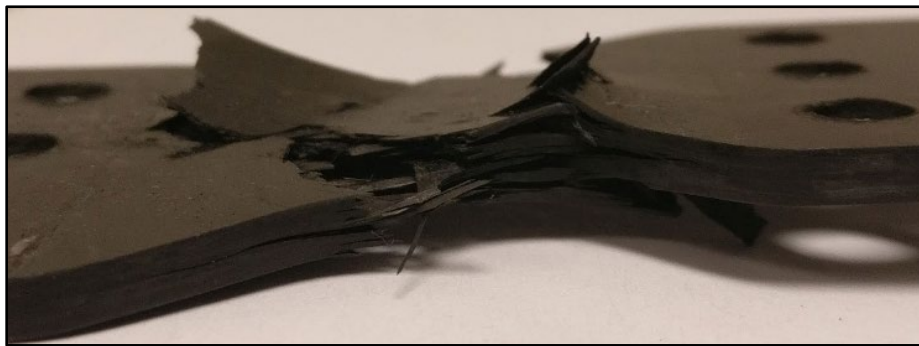
(c) Pure Shear Specimen – 90° Loading Angle

Figure 9: Failed fatigue specimens

Figure 10 shows through-thickness views of the 0 and 90° specimens. The failure modes observed in these specimens not only include fiber breakage and matrix cracking, but also significant amounts of delamination between the layers in the carbon fiber SMC-R specimens. A close-up view of the failure regions in fatigue specimens (Figure 11) depicts inter-fiber matrix cracking, fiber breakage and fiber pull-out in all three cases. In addition to these micro-failure modes, significant inter-laminar failures were observed under combined equal tension-shear and pure shear fatigue.



(a) Uniaxial Tension Specimen - 0° loading angle



(b) Pure Shear Specimen- 90° loading angle

Figure 10: Fatigue specimens exhibiting delamination

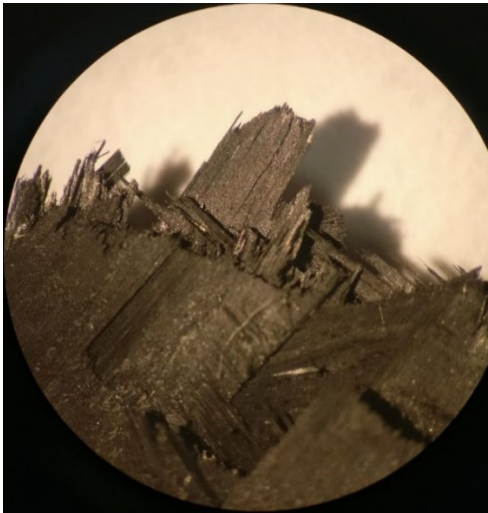
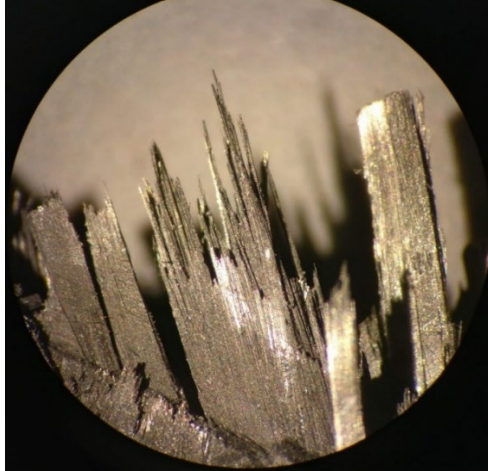


Figure 11: Close-up view of the failure regions of fatigue specimens

4 Analysis of Fatigue Test Data

Fatigue test results presented in Figure 7 show large scatter in fatigue life, which can be attributed to variations in fiber orientation and fiber distribution in the material. Similar observation has been made by several investigators [12, 14, 15, 17, 18] regarding scatter in the fatigue data of compression molded carbon fiber SMC-R composites. In this section, statistical analysis of fatigue data was conducted to predict the fatigue performance of the material. The best fit for the fatigue data was obtained using standard maximum likelihood methods. The statistical software MINITAB, version 17.3.1 was used to fit normal, log normal and Weibull distributions to the experimental data and Anderson-Darling test was used to determine the best fit lines. The data was right-censored at 1 million cycles to account for the run-out. The Weibull distribution showed a much better fit for the fatigue data compared to the normal and log normal distributions and was used to plot fatigue life diagrams at 90% and 50% reliabilities.

Figure 12 shows the Weibull probability distribution for specimens at 0° loading angle at maximum cyclic stress levels of 200 MPa. The y-axis in this figure represents the probability of failure and the x-axis represents the life in number of cycles to failure. Weibull plots shown in Figures 13 and 14 are for the 45 and 90° loading angle specimens at 110 MPa. The best fit lines obtained after conducting Anderson-Darling tests are also shown in Figures 12-14. It should be noted that in these Weibull plots, there are fewer data points for the 45 and 90° loading angles than for the 0° loading angle; therefore, the probability plots at these two loading angles may be considered less accurate than the probability plots at the 0° loading angle.

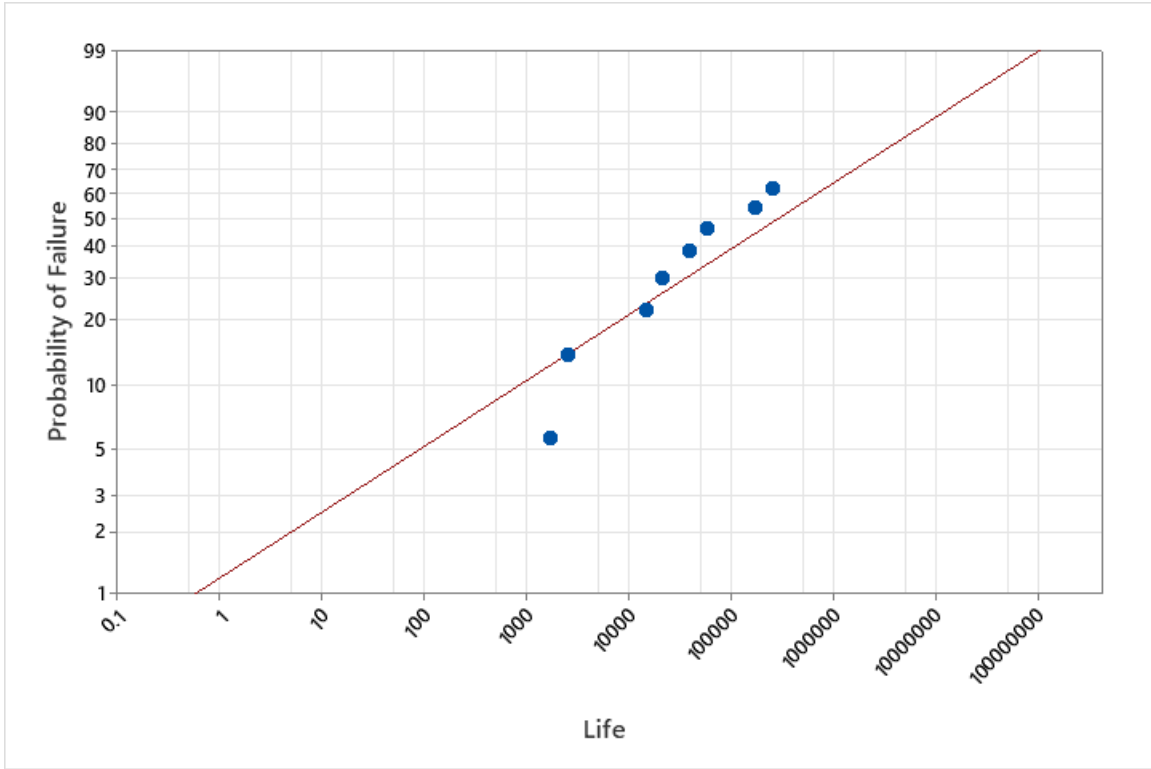


Figure 12: Weibull plot of life data of 0° specimens at 200 MPa maximum cyclic stress

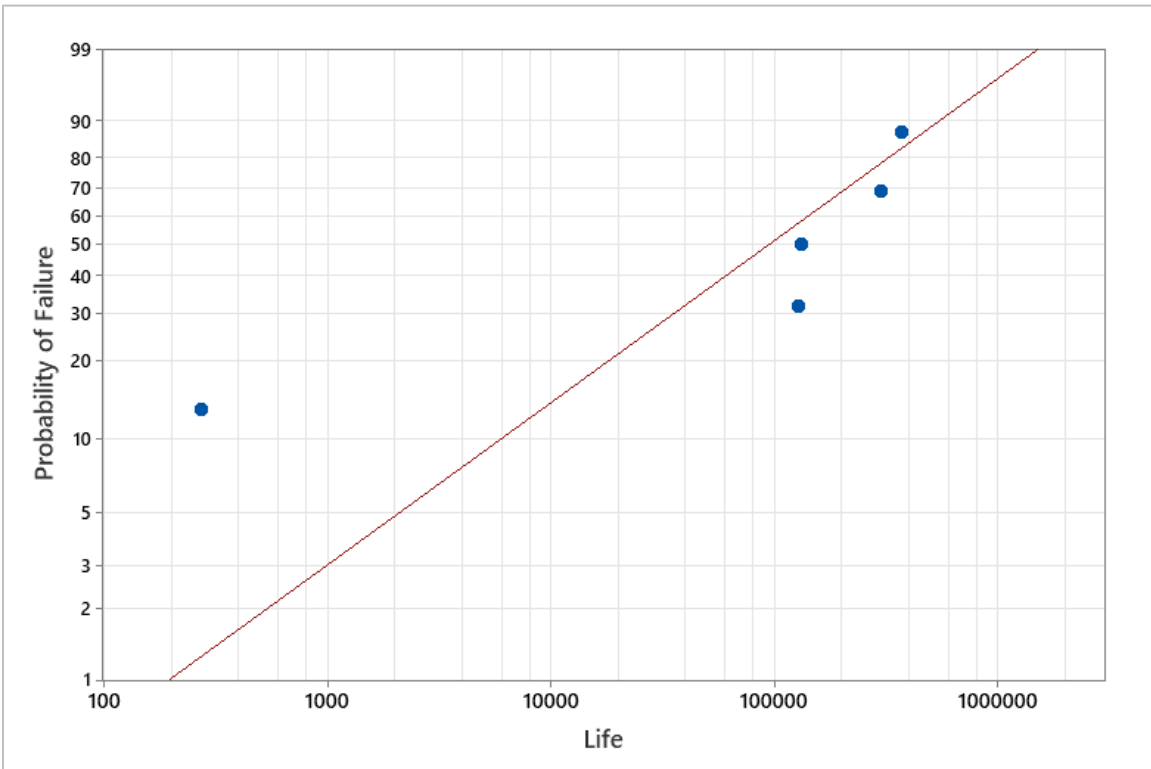


Figure 13: Weibull plot of life data of 45° specimens at 110 MPa maximum cyclic stress

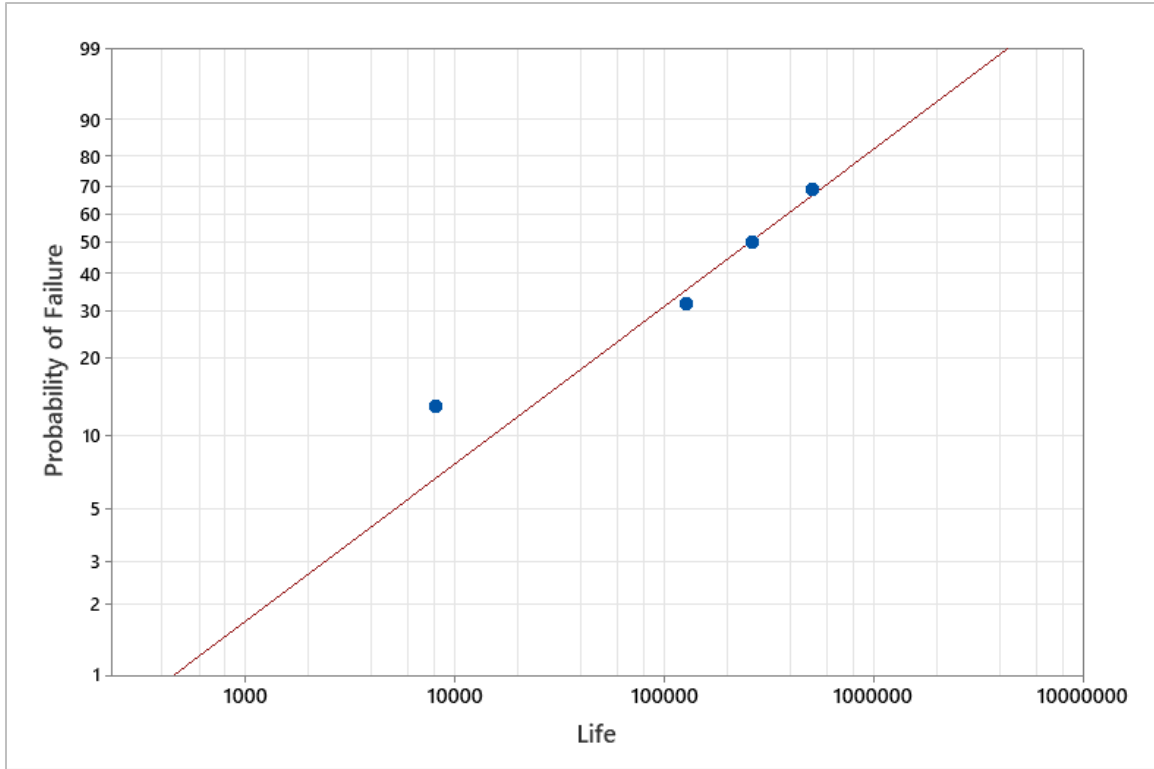


Figure 14: Weibull plot of life data of 90° specimens at 110 MPa maximum cyclic stress

Based on the Weibull analysis of the fatigue data, S-N curves of the material are plotted in Figures 15 and 16 under tension, pure shear, and combined equal tension and shear loading cases at 90% reliability and 50% reliability, respectively. The S-N curves under combined equal tension and shear loading is close to the S-N curve under shear loading, and both are much lower than the S-N curve under tension. It can be observed in these two figures that a linear relationship exists between the maximum cyclic stress and log (life). Table 3 lists the fatigue strength of the carbon fiber SMC-R at 10^6 cycles at 90 and 50% reliabilities. The fatigue strength-to-static strength ratios are also listed in Table 3. As can be observed in this table, as a percentage of static strength, the fatigue strength at 45° loading angle, i.e., under combined equal tension and shear is similar to the fatigue strength at 0° loading angle, i.e., under uniaxial tension. However, as a percentage of static shear strength, the fatigue strength in shear determined at 90° loading angle is much lower.

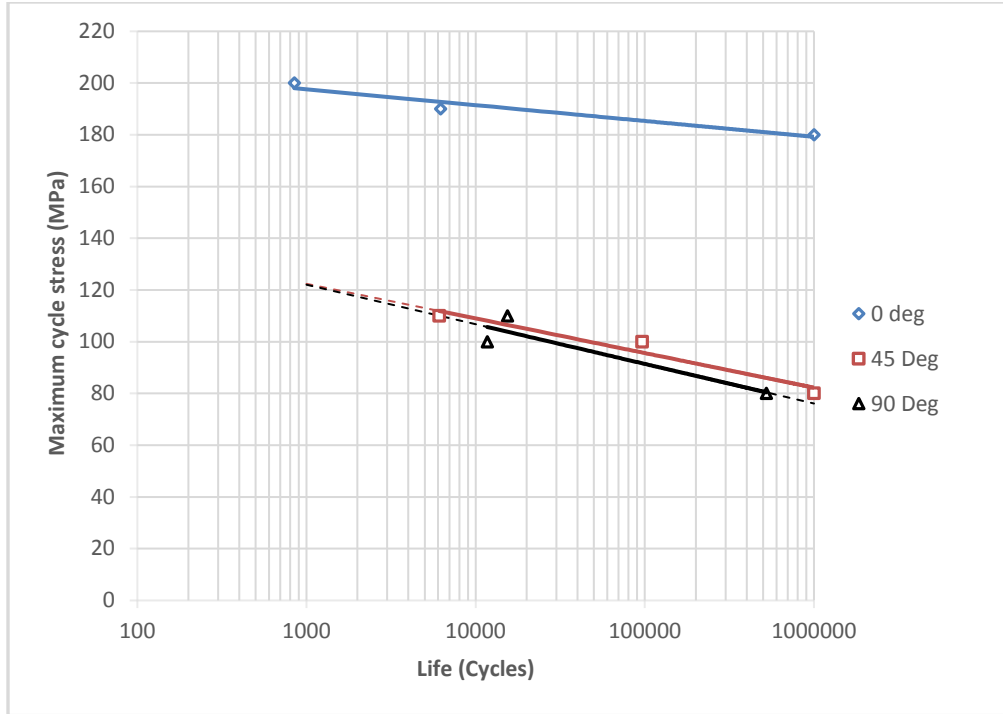


Figure 15: S-N curves carbon fiber SMC-R at 0, 45 and 90° loading angles at 90% reliability

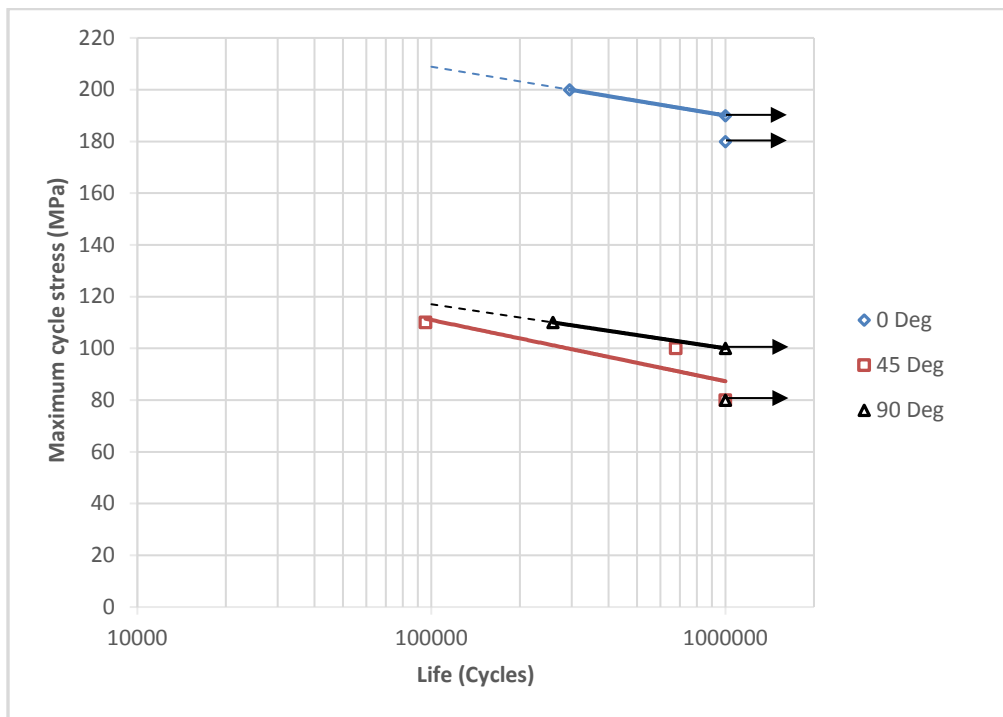


Figure 16: S-N curves carbon fiber SMC-R at 0, 45 and 90° loading angles at 50% reliability

Table 3: Fatigue strengths of carbon fiber SMC-R composite at three different loading angles

Loading Angle (°)	Mode of Loading	Fatigue Strength at 10^6 Cycles		Ratio of Fatigue Strength at 10^6 Cycles and Static strength	
		90% Reliability	50% Reliability	90% Reliability	50% Reliability
0	Uniaxial Tension	179.2	190	0.70	0.74
45	Equal Tension and Shear	82.2	87.2	0.66	0.70
90	Pure Shear	76.1	100	0.51	0.67

5 Conclusions

The static and fatigue behavior of a carbon fiber SMC-R composite were investigated under tension, shear, and combined tension-shear conditions. In biaxial conditions in which a shear stress is imposed along with a tensile stress, the tensile strength of the material decreases with increasing shear stress following a quadratic relationship. Since large variations were present in both static strength and fatigue life, statistical analysis was conducted using Weibull distribution to determine the mean static strengths and fatigue life at 90% and 50% reliabilities. The mean shear strength is 0.58 times the mean tensile strength. The von Mises equation is used to predict the static strength of the material under different ratios of tension and shear. It shows reasonably good agreement with experimentally determined strength data. The fatigue strength of the material under pure shear and combined equal tension and shear is much lower than the fatigue strength under pure tension. At 90% reliability, the fatigue strength at 1 million cycles is 70% of the static strength in tension loading and 66% under combined equal tension and shear loading. Under pure shear loading, the fatigue strength is about 51% of the static strength.

Acknowledgement

The authors acknowledge the help of Quantum Composites, a division of A. Schulman, of Midland, Michigan, USA for supplying the carbon fiber SMC-R plates used in this study.

References

- [1] D. Denton. SAE Technical Paper 790671, presented at the Passenger Car Meeting, Soc. of Auto. Eng., June 11-15, **1979**. <https://doi.org/10.4271/790671>
- [2] D. A. Reigner and B. A. Sanders, Proc. of National Technical Conference, Soc. of Plastics Eng., November **1979**.
- [3] S. S. Wang, E.S.-M Chim, T. P. Yu and D. P. Goetz, *J. Compos. Mater.*, **1983**, 17, 299-311. <https://doi.org/10.1177%2F002199838301700402>
- [4] T. Watanabe and M. Yasuda, *Composites*, **1982**, 13, 54-58. [https://doi.org/10.1016/0010-4361\(82\)90171-9](https://doi.org/10.1016/0010-4361(82)90171-9)
- [5] K. Y. Hour and H. Sehitoglu, *J. Compos. Mater.*, **1993**, 27, 782-805. <https://doi.org/10.1177%2F002199839302700803>
- [6] P. K. Mallick. *Polymer Composites*, **1981**, 2, 18-21. <https://doi.org/10.1002/PC.750020105>
- [7] S. S. Wang, and E. S.-M Chim, *J. Compos. Mater.*, **1983**, 17, 114-134. <https://doi.org/10.1177%2F002199838301700203>
- [8] S. S. Wang, and E. S.-M. Chim, and N. M. Zahlan, *J. Compos. Mater.*, **1983**, 17, 250-266. <https://doi.org/10.1177%2F002199838301700306>
- [9] G. Lamanna and A. Ceparino. *Open Mater. Sci. J.*, **2014**, 8, 108-113. <https://dx.doi.org/10.2174/1874088X01408010108>
- [10] P. Feraboli, E. Peitso, F. Deleo, T. Cleveland and P. B. Steckler, *J. Compos. Mater.*, **2009**, 43, 1947-1965. <https://doi.org/10.1177%2F0021998309343028>
- [11] P. Feraboli, E. Peitso, F. Deleo, T. Cleveland and P. B. Steckler, *J. Rein. Plast. Compos.*, **2009**, 28, 1191-1214. <https://doi.org/10.1177%2F0731684408088883>
- [12] P.S. Stelzer, T. Hebertinger, V. Reisecker, J. Maier and Z, Proc American Soc for Composites, 35th Technical Conference, New York, NY, **2021**. <https://doi.org/10.12783/asc35/34868>
- [13] L. M. Martulli, L. Muyshondt, M. Kerschbaum, S. Pimenta, S.V. Lomov and Y. Swolfs. *Compos. A.*, Vol. 126, 2019. <https://doi.org/10.1016/j.compositesa.2019.105600>
- [14] L. M. Martulli, L. Muyshondt, M. Kerschbaum, S. Pimenta, S.V. Lomov and Y. Swolfs, *Int. J. Fatigue*, **2020**, 134. <https://doi.org/10.1016/j.ijfatigue.2020.105510>
- [15] H. Tang, Z. Chen, G. Zhou, et al., *Int. J. Fatigue*, **2019**, 125, 394-405. <https://doi.org/10.1016/j.ijfatigue.2019.04.016>
- [16] H. Tang, G. Zhou, Z. Chen, et al., *Compos. Struct.*, **2019**, 215, 85-97.

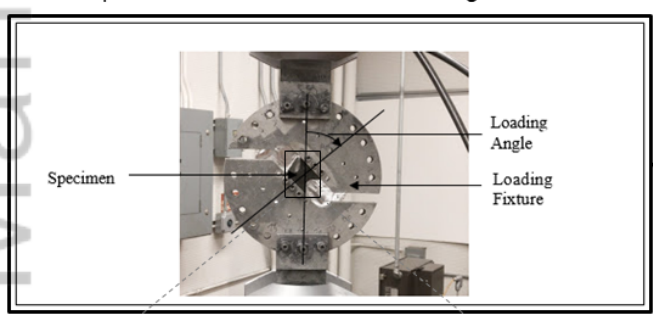
<https://doi.org/10.1016/j.compstruct.2019.02.041>

- [17] C. Nony-Davadie, L. Peltier, Y. Chemisky, B. Surowiec and F. Meraghini, *J. Compos. Mater.*, **2019**, 53, 1437-1457. <https://doi.org/10.1177%2F0021998318804612>
- [18] S. Sieberer, S. Nonn and M. Schagerl, *Int. J. Fatigue*, **2020**, 131. <https://doi.org/10.1016/j.ijfatigue.2019.105289>
- [19] M. Arcan, Z. Hashin and A. Voloshin, *Exp. Mech.*, **1978**, 18, 141-146. <https://doi.org/10.1007/BF02324146>
- [20] A. Voloshin and M. Arcan. *Fibre Sci. Tech.*, **1980**, 13, 125-134. [https://doi.org/10.1016/0015-0568\(80\)90041-X](https://doi.org/10.1016/0015-0568(80)90041-X)
- [21] R. Mandapati and P. K. Mallick, Proc. 20th International Conference on Composite Mater, July 19-24, **2015**.
- [22] P. B. Gning, D. Delsart, J. M. Mortier and D. Coutellier, *Compos. B*, **2010**, 41, 308-316. <https://doi.org/10.1016/j.compositesb.2010.03.004>
- [23] M. Urapakam Ramakrishnan and P. K. Mallick, *Compos. B*, **2019**, 176, 107-141. <https://doi.org/10.1016/j.compositesb.2019.107141>
- [24] R. Mandapati, Study of Biaxial Fatigue Behavior of Fiber Reinforced Polymer under Tensile and Shear Loadings, Ph.D. Dissertation, Automotive Systems Engineering, University of Michigan-Dearborn, Dearborn, MI, **2016**. <https://hdl.handle.net/2027.42/136076>
- [25] K. C. Kapur and L. R. Lamberson, *Reliability in Engineering Design*, John Wiley & Sons, NY, **1977**.
- [26] P. K. Mallick, *Fiber-Reinforced Composites*, 3rd ed. CRC Press, **2008**.
- [27] R. Hill, *The Mathematical Theory of Plasticity*, Clarendon Press, **1950**.

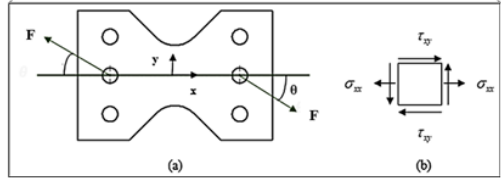
Static and Fatigue Behavior of a Carbon-Fiber SMC-R Composite under Combined Tensile and Shear Stresses

Monish Urapakam Ramakrishnan, Pankaj K. Mallick
University of Michigan-Dearborn

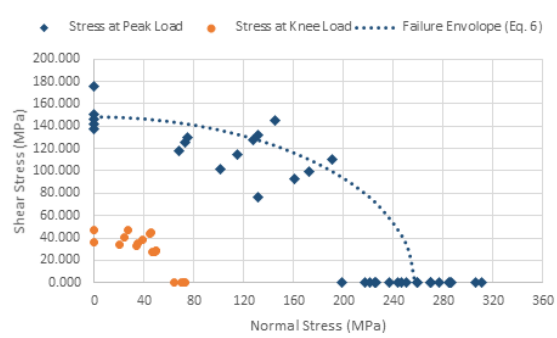
Experimental setup for a butterfly shaped Arcan specimen mounted on the MTS testing machine



Schematic of load acting on a specimen (a) and stress element at significant section (b)



Static Results



90%R Fatigue Results

